© 2016. Published by The Company of Biologists Ltd | Development (2016) 143, 75-87 doi:10.1242/dev.124461

RESEARCH ARTICLE

Two classes of matrix metalloproteinases reciprocally regulate synaptogenesis

Mary Lynn Dear, Neil Dani, William Parkinson, Scott Zhou and Kendal Broadie*

ABSTRACT

Synaptogenesis requires orchestrated intercellular communication between synaptic partners, with trans-synaptic signals necessarily traversing the extracellular synaptomatrix separating presynaptic and postsynaptic cells. Extracellular matrix metalloproteinases (Mmps) regulated by secreted tissue inhibitors of metalloproteinases (Timps), cleave secreted and membrane-associated targets to sculpt the extracellular environment and modulate intercellular signaling. Here, we test the roles of Mmp at the neuromuscular junction (NMJ) model synapse in the reductionist *Drosophila* system, which contains just two Mmps (secreted Mmp1 and GPI-anchored Mmp2) and one secreted Timp. We found that all three matrix metalloproteome components co-dependently localize in the synaptomatrix and show that both Mmp1 and Mmp2 independently restrict synapse morphogenesis and functional differentiation. Surprisingly, either dual knockdown or simultaneous inhibition of the two Mmp classes together restores normal synapse development, identifying a reciprocal suppression mechanism. The two Mmp classes co-regulate a Wnt trans-synaptic signaling pathway modulating structural and functional synaptogenesis, including the GPI-anchored heparan sulfate proteoglycan (HSPG) Wnt co-receptor Dally-like protein (Dlp), cognate receptor Frizzled-2 (Frz2) and Wingless (Wg) ligand. Loss of either Mmp1 or Mmp2 reciprocally misregulates Dlp at the synapse, with normal signaling restored by co-removal of both Mmp classes. Correcting Wnt co-receptor Dlp levels in both Mmp mutants prevents structural and functional synaptogenic defects. Taken together, these results identify an Mmp mechanism that fine-tunes HSPG co-receptor function to modulate Wnt signaling to coordinate synapse structural and functional development.

KEY WORDS: Synaptomatrix, Trans-synaptic signaling, Heparan sulfate proteoglycan, Wnt, Neuromuscular junction, *Drosophila*

INTRODUCTION

Development of a communicating junction between a presynaptic neuron and its postsynaptic target requires coordinated signaling between synaptic partner cells. Bidirectional trans-synaptic signals modulate synaptogenesis by traversing a specialized extracellular environment (the 'synaptomatrix'; Dani and Broadie, 2012; Vautrin, 2010). Matrix metalloproteinases (Mmps) are a conserved family of secreted and membrane-anchored extracellular proteases that regulate developmental processes by cleaving membrane proteins, secreted signaling ligands and extracellular matrix (ECM) components to inhibit, activate, sequester, release or expose cryptic sites, thereby sculpting the extracellular environment and modulating intercellular signaling (Kessenbrock et al., 2010; Page-McCaw et al., 2007; Sternlicht and Werb, 2001). Mammalian Mmps have known roles in neurogenesis, axon guidance, dendritic development, synaptic plasticity and behavioral outputs, but mechanisms remain elusive and roles in synaptogenesis are under-studied (Huntley, 2012). In mice, 24 Mmps regulated by four Timps make genetic studies challenging, with extensive functional redundancy and compensation (Page-McCaw et al., 2007). By contrast, the *Drosophila* genome encodes just one secreted Mmp (Mmp1), one membrane Mmp (GPI-anchored Mmp2) and one secreted Timp. In lieu of mammalian studies, which show that extracellular proteases play central roles determining synapse structure, function and number (reviewed in Reinhard et al., 2015; Shinoe and Goda, 2015; Wójtowicz et al., 2015), we took advantage of the reductionist *Drosophila* model to genetically dissect the complete, integrated mechanism of the matrix metalloproteome in synaptic development.

Drosophila Mmps display canonical structure and function, with a cleavable prodomain that modulates enzyme latency, a zinc-dependent catalytic domain and hemopexin domain (Llano et al., 2000, 2002; Page-McCaw et al., 2003). *Drosophila* Timp resembles mammalian Timps in structure and function. *Drosophila* Timp inhibits mammalian Mmps and mammalian Timps inhibit *Drosophila* Mmps, demonstrating an evolutionarily conserved function (Llano et al., 2000; Wei et al., 2003). Like the roles of mouse Mmps in neurodevelopment, *Drosophila* Mmps have been shown to regulate embryonic axonogenesis, BMP-dependent motor axon pathfinding and dendritic remodeling in larval sensory neurons (Kuo et al., 2005; Miller et al., 2008, 2011; Yasunaga et al., 2010). Importantly, mammalian Mmps are upregulated in neurological disorders (Huntley, 2012), including multiple sclerosis (Agrawal et al., 2008), epilepsy (Pollock et al., 2014; Wilczynski et al., 2008) and Fragile X syndrome (FXS), the most common heritable determinant of intellectual disability and autism spectrum disorders (Gatto and Broadie, 2011). Similar to the mouse FXS model (Bilousova et al., 2009; Sidhu et al., 2014), the *Drosophila* FXS disease model exhibits Mmp dysfunction as an underlying cause of neurodevelopmental phenotypes (Siller and Broadie, 2012). Neural defects in the *Drosophila* FXS model, including impairments in both morphological and functional synaptic differentiation (Doll and Broadie, 2014) are remediated by pharmacological or genetic Mmp inhibition (Siller and Broadie, 2011).

In the *Drosophila* FXS disease model, synaptogenic defects have been causally linked to heparan sulfate proteoglycan (HSPG) Dally-like protein (Dlp) co-receptor misregulation of the Wnt Wingless (Wg) trans-synaptic signaling that drives synaptogenesis (Friedman et al., 2013). Does the function of Mmp intersect with this established synaptogenic mechanism? The findings in this

Department of Biological Sciences, Kennedy Center for Research on Human Development, Vanderbilt University, Nashville, TN 37235-1634, USA.

*Author for correspondence (kendal.broadie@vanderbilt.edu)

Received 17 March 2015; Accepted 18 November 2015

Development (2016) 143, 75-87 doi:10.1242/dev.124461

study support the model that synapse development requires a precise balance of Mmp activities from both presynaptic and postsynaptic partner cells. The results also show that the two Mmps (secreted Mmp1 and GPI-anchored Mmp2) bidirectionally regulate Dlp to modulate Wg trans-synaptic signaling. Both Mmp functions inhibit structural and functional synaptogenesis, suggesting that Dlp can act as both a positive and negative regulator of synapse development.

RESULTS

Mmp1 and Mmp2 both regulate synapse morphogenesis

We first asked whether the two *Drosophila* Mmps affect morphological synaptogenesis at the well-characterized glutamatergic neuromuscular junction (NMJ). Each NMJ terminal contains a fairly stereotypical array of synaptic boutons, each containing large synaptic vesicle reserves and multiple active zone release sites (Menon et al., 2013). To test Mmp requirements in NMJ structural development, we assayed a wide range of single mutant, double mutant and targeted transgenic conditions (Fig. 1, Table S1A). Both *mmp1* and *mmp2* loss-of-function (LOF) mutants displayed a significant, 25-40% increase in synaptic bouton number (Fig. 1A,B, 'single *mmp* LOF') compared with matched genetic controls, indicating that Mmp1 and Mmp2 both restrict synaptic structural development. In addition, only *mmp1* mutant boutons were significantly smaller in size (Fig. 1A, Table S1B). Surprisingly, both Mmp heterozygotes (*mmp1*/+ and *mmp2*/+) similarly show a striking increase in bouton number, comparable in magnitude to the Mmp homozygous mutants (Fig. S1D, Table S1A). Ubiquitous (*UH1*) mmp^{RNAi} for both Mmp classes produced similar increases in bouton number compared with LOF mutants (Fig. 1B, cell-targeted mmp^{RNAi}), with measured protein knockdown levels that were also comparable to the corresponding mutants (Fig. S7).

To test for stronger effects, we wanted to assay simultaneous removal of Mmp1 and Mmp2. However, Mmp double mutants are early larval lethal and the few animals that survive to early third instar are much smaller than matched controls. We therefore used double $mmp1^{RNAi}$; $mmp2^{RNAi}$ knockdown (*UH1>mmp1+2*^{RNAi}) and Timp overexpression (*UH1>Timp*), as two independent means of blocking the functions of both Mmps simultaneously. Both Mmp blocking conditions individually display 100% penetrant late larval/early pupal lethality; together they represent the most severe double Mmp LOF conditions available for these studies. Astonishingly, neither *UH1>mmp1+2*^{RNAi} nor *UH1>Timp* resulted in the predicted additive effect but, unexpectedly, displayed architecturally normal NMJs (Fig. 1A; Table S1A). In the first test, *UH1>mmp1+2*^{RNAi} produced NMJ bouton numbers that were comparable to the control and were significantly reduced compared with the supernumerary boutons present in both single RNAi conditions (Fig. 1B, 'double *mmp* inhibition'). Likewise,

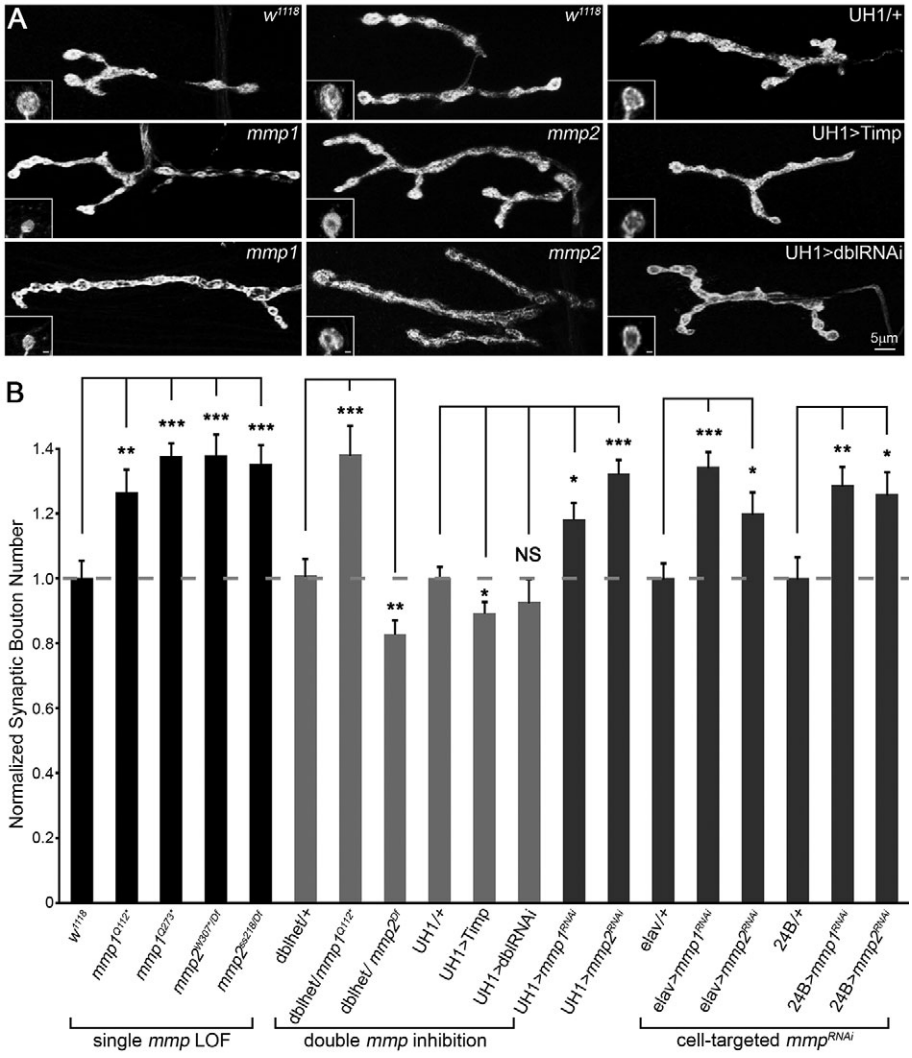

Fig. 1. Mmp1 and Mmp2 repress NMJ structural development. (A) Black and white images of NMJs co-labeled for synaptic markers HRP and Dlg in *mmp1* (middle row: $mmp1^{Q112*}$ and bottom row: $mmp1^{Q273*}$), *mmp2* (middle row: $mmp2^{W307*/Df}$ and bottom row: $mmp2^{ss218/Df}$) and two double *mmp* inhibition conditions [*UH1>Timp* and *UH1>mmp1+2*^{RNAi} (*UH1>dblRNAi*)], compared with controls (top row). Insets show high magnification single boutons. Scale bars: 1 µm. (B) Quantified bouton number for denoted genotypes normalized to genetic controls. Genotypes clustered by single *mmp* loss-of-function (LOF; left), double inhibition (middle) and cell-targeted RNAi knockdown in neurons (*elav*) or muscle (*24B*) for both genes (right). Double inhibition includes double *mmp1,mmp2* heterozygous condition (dblhet), *UH1>Timp* and *UH1>mmp1+2*^{RNAi} (dblRNAi). See Fig. S1 for additional genotypes. See Table S1A for raw data values and sample sizes.

Development (2016) 143, 75-87 doi:10.1242/dev.124461

UH1>Timp NMJ architecture closely resembled matched genetic controls (Fig. 1A), with only a subtle 10% reduction in synaptic bouton number (Fig. 1B, 'double inhibition'). Moreover, double *mmp* heterozygotes ($mmp2^{W307*/+}$, $mmp1^{Q112*/+}$; dblhet) also showed no significant difference in bouton number compared with controls, and thus suppressed the overgrowth characterizing both single *mmp* heterozygotes alone (Fig. 1B, 'double inhibition', Table S1A). Consistently, postsynaptic Timp overexpression (*24B>Timp*) was sufficient to suppress the elevated bouton number in both single *mmp* heterozygotes back to control levels (Fig. S1B,C). Collectively, these results indicate a co-suppressive interplay between the two Mmp classes and strongly suggest that the Mmp ratio is a critically important determinant of synapse structure.

To further test this interaction, we sought to genetically reduce Mmp levels in a dose-dependent manner (Fig. 1B, 'double inhibition', Table S1A). Using the *mmp* double heterozygote condition as a baseline, we sequentially removed additional *mmp* gene copies (Fig. 1B, 'double inhibition'). The Mmp imbalance caused by removal of *mmp1* ($mmp2^{W307*/+}$, $mmp1^{Q112*/Q112*}$) resulted in a ~40% increase in synaptic bouton number and the converse removal of *mmp2* ($mmp2^{W307*/Df}$, $mmp1^{Q112*/+}$) significantly reduced bouton number (Fig. 1B, 'double inhibition'). These results support an Mmp suppression model, and indicate that development of NMJs requires a precise balance of Mmp1:Mmp2 activities. Consistent with the interpretation that Mmp balance is crucial, all rescue attempts with UAS-*mmp* transgenes resulted in lethality.

To dissect the tissue-specific requirements for NMJ structural development, we used cell-targeted RNAi to knock down Mmp classes singly (mmp^{RNAi}) and in combination ($mmp1{+}2^{RNAi}$) in either neurons (*elav*) or muscles (*24B*; also known as *how*) (see Table S3A for knockdown levels). Consistent with the model, reducing each single Mmp class alone either presynaptically or postsynaptically caused a significant increase in synaptic bouton number (Fig. 1B, 'cell-targeted mmp^{RNAi}'). Importantly, the double $mmp1{+}2^{RNAi}$ phenotype within either muscle or neuron was stronger than either single mmp^{RNAi} alone (Fig. S1A,C; Table S1A). Conversely, simultaneous knockdown in neurons and muscles of each Mmp alone using a novel combined driver (*elav,24B>*mmp^{RNAi}) caused a robust increase in bouton differentiation, which also failed to occur in the *elav,24B>*$mmp1{+}2^{RNAi}$ double knockdown condition (Fig. S1A,C, Table S1A). These results clearly show that proper NMJ differentiation requires both Mmp classes in both pre- and postsynaptic cells, and indicate that Mmp1+2 (neuron): Mmp1+2 (muscle) ratios across both cell types must be balanced for proper structural morphogenesis.

Mmp1 and Mmp2 both regulate differentiation of synapse function

Structural and functional synaptic development occurs simultaneously, but they are regulated independently by distinct molecular mechanisms. To test how Mmps might contribute to NMJ functional development, nerve stimulation evoked excitatory junction currents (EJCs) were quantified as a measure of neurotransmission strength (Fig. 2, Table S2A). Both Mmp1 and Mmp2 negatively regulate functional differentiation, resulting in clearly elevated neurotransmission in all single Mmp mutants (Fig. 2A). The range of Mmp single mutants showed highly significant 25-65% increased EJC amplitudes compared with matched genetic controls (Fig. 2B, 'single *mmp* LOF', Table S2A). Conversely, *UH1>Timp* showed significantly reduced neurotransmission. Similarly, *UH1>*$mmp1{+}2^{RNAi}$ completely suppressed the elevated EJC amplitudes characterizing both single *UH1>*mmp^{RNAi} conditions, with neurotransmission significantly reduced ~25% compared with controls (Fig. 2A,B). These results suggest that Mmp1 and Mmp2 might also co-suppress NMJ functional differentiation. Postsynaptic, but not presynaptic, targeted *mmp* knockdown of both classes caused significantly increased EJC amplitudes, indicating that Mmp1 and Mmp2 are required only from the muscle for functional regulation (Fig. 2B, 'cell-targeted mmp^{RNAi}'). However, both Mmps function extracellularly and homeostatic mechanisms between synaptic partners act trans-synaptically; thus, the underlying mechanism regulating neurotransmission strength might not be cell-autonomous (Davis and Müller, 2015).

To further investigate how Mmps regulate functional differentiation, we next assayed spontaneous neurotransmission by quantifying miniature EJC (mEJC) frequency and amplitude as measures of pre- and postsynaptic machinery, respectively (Fig. S2, Table S2B) (Dani et al., 2012). Presynaptically, we found that *mmp2* LOF mutants exhibited a robust ~80% increase in mEJC frequency (Fig. S2A,B). Postsynaptically, *mmp1* LOF mutants showed a significant ~30% increase in mEJC amplitude, whereas *mmp2* LOF mutants displayed a ~15% decrease in mEJC amplitude (Fig. S2A,B). Importantly, there were no detectable changes in mEJC amplitude or frequency in UH1>$mmp1{+}2^{RNAi}$ double knockdown animals (Fig. S2). In calculating quantal content to measure the level of synaptic vesicle release, *mmp2* mutants had a ~twofold increase, whereas *mmp1* mutants showed no significant change compared with controls (Fig. S2B). In the *UH1>*$mmp1{+}2^{RNAi}$ double loss condition, quantal content was decreased by ~35%. It is noted that there are inconsistencies between Mmp LOF mutant and mmp^{RNAi} mEJC phenotypes (Table S2B). Nevertheless, the results clearly demonstrate that Mmp1 and Mmp2 regulate different aspects of NMJ functional development.

Mmp1 and Mmp2 both regulate synapse molecular assembly

NMJ function is regulated by the number and composition of postsynaptic glutamate receptors (GluRs) juxtaposing presynaptic active zone glutamate release sites (Menon et al., 2013). Since both evoked and spontaneous neurotransmission are altered in Mmp mutants, we next tested how the two Mmp classes might regulate molecular synaptic assembly by quantifying both presynaptic Bruchpilot (Brp) containing active zones (Wagh et al., 2006) and postsynaptic GluR domains (Qin et al., 2005). On the presynaptic side, both *mmp1* and *mmp2* LOF mutants had significantly more Brp-containing active zones (puncta/μm^3) compared with matched controls (Fig. S3C, Table S2C). On the postsynaptic side, *mmp1* LOF mutants had more domains containing the essential GluRIID subunit (Qin et al., 2005) measured as puncta/μm^3, whereas *mmp2* LOF mutants showed a smaller, non-significant increase in GluR puncta density (Fig. S3, Table S2C). No defects were detected in the apposition between synaptic compartments in either *mmp1* or *mmp2* mutants, as all Brp-positive active zones juxtaposed a GluRIID cluster (Table S2C). Importantly, no defects in either presynaptic active zones or postsynaptic GluR domains were detected in *UH1>*$mmp1{+}2^{RNAi}$ animals (Fig. S3).

Each GluR tetramer contains either a GluRIIA or GluRIIB variable subunit modulated by distinct regulatory mechanisms (Chen and Featherstone, 2005; Diantonio et al., 1999). Subunit selection dictates distinctive receptor functional properties (Qin et al., 2005); for example, A-type GluRs mediate increased postsynaptic sensitivity and B-Type GluRs rapidly desensitize.

Development (2016) 143, 75-87 doi:10.1242/dev.124461

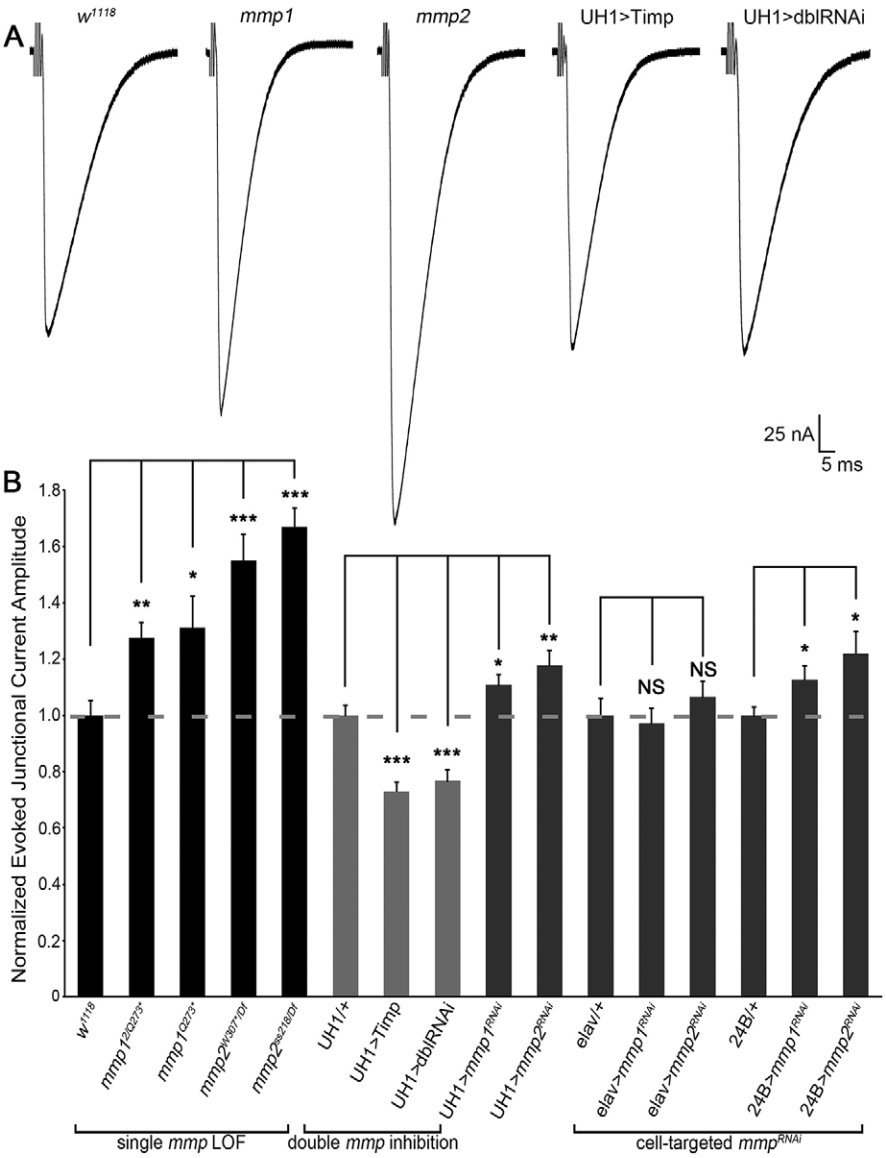

Fig. 2. Mmp1 and Mmp2 repress functional differentiation of the NMJ. (A) NMJ electrophysiology two-electrode voltage-clamp (TEVC) records showing motor nerve stimulation evoked excitatory junctional currents (EJCs) from genetic control (w^{1118}), $mmp1^{2/Q273*}$, $mmp2^{ss218/Df}$, *UH1>Timp* and *UH1>mmp1+2*^{RNAi} (dblRNAi). (B) Quantified EJC amplitudes for denoted genotypes normalized to genetic controls. See Fig. S2 for mEJC analyses. See Table S2 for raw data values and sample sizes. **P*<0.05, ***P*<0.01, ****P*<0.001; NS, not significant.

The *mmp2* LOF mutants displayed significantly more GluRIIA puncta/μm^3, although the overall fluorescence signal intensity was slightly decreased (Fig. S4, Table S3C). Conversely, *mmp1* mutants showed a non-significant increase in GluRIIA puncta/μm^3, with overall signal intensity significantly increased compared with controls (Fig. S4, Table S3C). For GluRIIB, both *mmp1* and *mmp2* mutants showed significantly increased puncta/μm^3, with signal intensity decreased in the *mmp1* mutants alone (Fig. S5, Table S3C). These GluR alterations likely confer the increased functional neurtransmission properties characterizing the Mmp LOF mutants (Fig. 2, Fig. S2) (Marrus and DiAntonio, 2004). These results show that Mmp1 and Mmp2 have distinct roles negatively regulating synaptic molecular assembly.

Drosophila NMJ synaptic ultrastructure is particularly well-characterized, with functionally and spatially defined synaptic vesicle pools organized around presynaptic active zones (containing an electron-dense T-bar) and the muscle subsynaptic reticulum (SSR) molded into elaborate membrane folds (Dani et al., 2014; Long et al., 2010). We therefore next examined Mmp roles in NMJ ultrastructural development using transmission electron microscopy (TEM), with the prediction that *mmp2* mutants would show presynaptic defects aligning with the previously observed functional phenotypes (Fig. 3, Table S1B). As Mmps have well established roles in ECM degradation, we were surprised to find that synaptic ultrastructure were largely normal in both Mmp mutants, with no detectable deficits in: (1) the architecture of the active zone or T-bar; (2) the appearance or width of the synaptic cleft; and (3) SSR folding or density (Fig. 3A; Table S1B). Similar to bouton volume confocal measurements, bouton cross-sectional area was significantly reduced by ~50% in *mmp1* mutants (Fig. 3A,B). The *mmp2* LOF mutants had significantly increased synaptic vesicle number/density (Fig. 3A,B), agreeing with elevated mEJC frequency (Fig. S2). Synaptic vesicle density at the active zone (<250 nm from T-bar; Rohrbough et al., 2007) and in the reserve domain (250-500 nm from T-bar; Mohrmann et al., 2008) was elevated in *mmp2* single mutants, with a similar non-significant trend in *mmp1* mutants (Fig. 3A,B). Again, these phenotypes were not present in *UH1>mmp1+2*^{RNAi} animals. Lack of any gross abnormalities in the matrix or SSR suggest that Mmps at the synapse function in the synaptomatrix to actively modulate intercellular signaling interactions between neurons and muscle, rather than permissive proteases degrading physical barriers, such as structural ECM components.

Development (2016) 143, 75-87 doi:10.1242/dev.124461

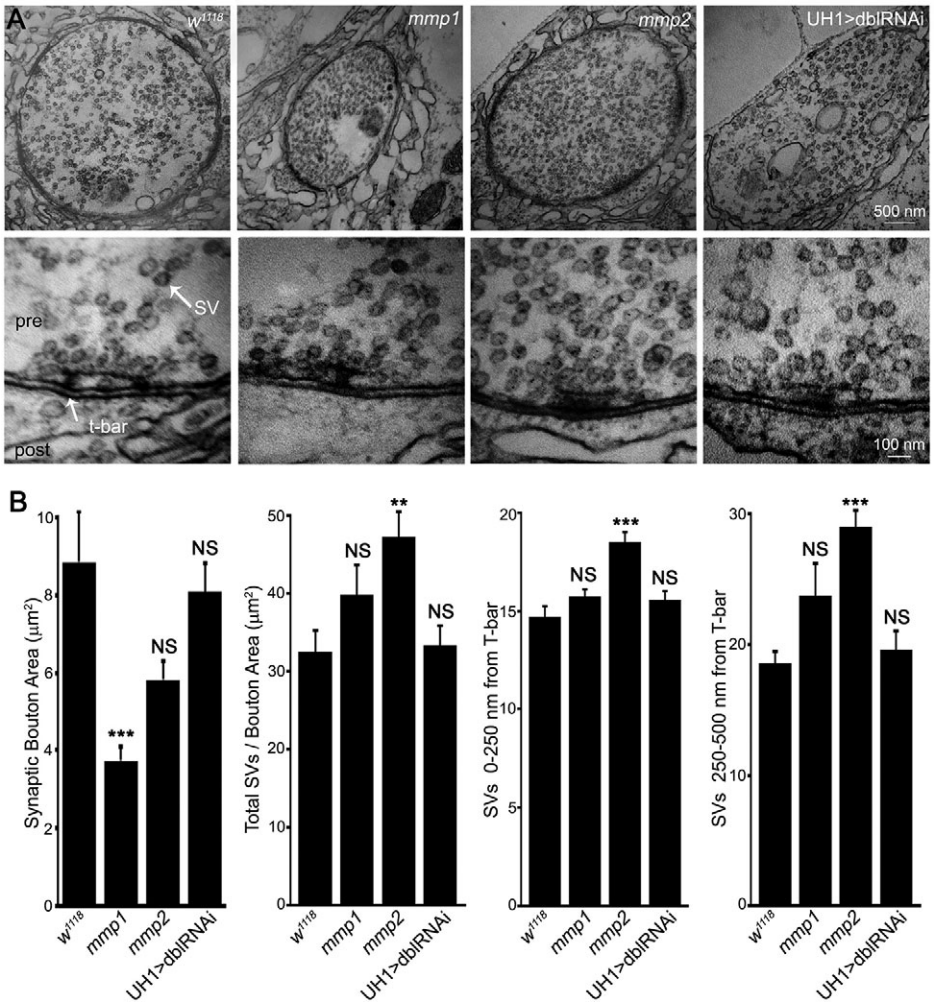

Fig. 3. Mmp1 and Mmp2 modulate synaptic ultrastructural development.
(A) Transmission electron microscopy (TEM) images of NMJ boutons (low magnification, top) and presynaptic active zones (high magnification, bottom) in control (w^{1118}), $mmp1^{Q112*/Q273*}$, $mmp2^{ss218/Df}$ and *UH1>mmp1+2*^{RNAi} (dblRNAi).
(B) Quantification of ultrastructural bouton area, synaptic vesicle (SV) number/bouton area, and SV number within 0-250 and 250-500 nm of active zone T-bars. See Table S1B for data values and sample sizes. See Figs S3-S5 for analyses of pre- and postsynaptic molecular components. ***P*<0.01, ****P*<0.001; NS, not significant.

Mmp1, Mmp2 and Timp co-dependently localize to the NMJ synaptomatrix

Our working model proposes that Mmp1, Mmp2 and their Timp inhibitor all co-localize extracellularly to the NMJ synapse. We therefore next examined expression of this three-component matrix metalloproteome in wild-type and mutant backgrounds. Prior efforts have produced Mmp1 antibodies (Page-McCaw et al., 2003), which we previously used to reveal localization of Mmp1 to the NMJ (Siller and Broadie, 2011) as confirmed here (Fig. S6A, Fig. S7A,D). Two Mmp2 antibodies exist that work on western blots (Jia et al., 2014; Wang et al., 2010), but neither is effective for immunocytochemistry. No *Drosophila* Timp antibody has been reported. We therefore generated new antibodies against both *Drosophila* Mmp2 and Timp that work for both immunocytochemistry and western blot analyses (Fig. 4, Figs S6-S8).

Western blot studies showed that the antibody against Mmp2 specifically recognized a ~90 kDa band in larvae of the predicted Mmp2 molecular mass, as well as three weaker bands (~120, 85 and 76 kDa) in isolated neuromusculature (Fig. 4G, Fig. S6B). The antibody against Timp specifically recognized a ~28 kDa band at the predicted Timp molecular mass, which increased with *UH1*>Timp and was absent in *timp*-null mutants (Fig. S6C). In tissue immunocytochemistry, Mmp1, Mmp2 and Timp labeling were all dramatically reduced in respective single LOF mutants as well as with single *UH1>mmp*^{RNAi} conditions (Fig. S7, Table S3A,B). Importantly, *UH1>mmp1+2*^{RNAi} eliminated Mmp1 and Mmp2 expression at the NMJ (Fig. S7A,B), comparable to quantified protein levels at corresponding single *UH1>mmp*^{RNAi} and genetic LOF mutant NMJs (Fig. S7D,E). As previously described (Siller and Broadie, 2011), detergent-free immunohistochemistry showed that Mmp1 localized to the extracellular space within the perisynaptic domain at the NMJ and was particularly enriched around synaptic boutons (Fig. S7A, Fig. S8A). Similarly, extracellularly labeled Mmp2 had a closely overlapping expression pattern, but was more restricted to the bouton surface, as predicted for a membrane-tethered protein (Fig. S7B, Fig. S8B). Finally, detergent-free labeling showed that Timp was highly enriched at the NMJ surrounding boutons in the extracellular synaptomatrix, albeit with a slightly more diffuse pattern, as predicted for a smaller secreted protein (Fig. S7C, Fig. S8C). Thus, all three proteins of the tripartite matrix metalloproteome overlap at the NMJ synapse.

With these new antibody tools and knowledge of Mmp1, Mmp2 and Timp expression at the synapse, we next addressed interactive changes (Fig. 4, Table S3A,B). Under detergent-free conditions, all three proteins were examined for extracellular expression in the respective Mmp LOF mutant and *UH1>Timp* conditions. First, imaging for Mmp1 expression using the antibodies specific for the catalytic domain (Page-McCaw et al., 2003) revealed significant increases in Mmp1 levels in *mmp2* LOF mutants and, conversely, significant decreases in Mmp1 at *UH1>Timp* NMJs (Fig. 4A,B, Table S3A). By contrast, Mmp2 was significantly decreased in *mmp1* LOF mutants and also moderately decreased at *UH1>Timp*

Development (2016) 143, 75-87 doi:10.1242/dev.124461

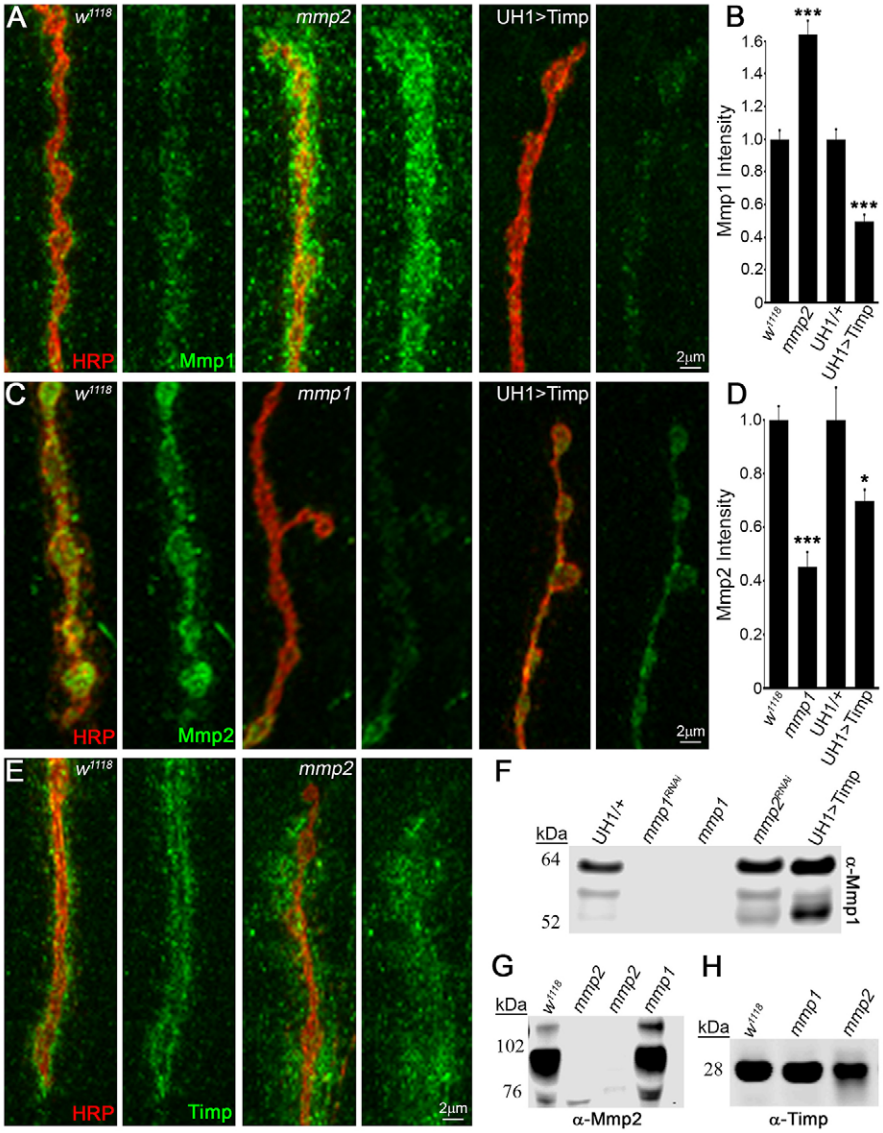

Fig. 4. Mmp1, Mmp2 and Timp exhibit co-dependent synaptic localization. (A) NMJ extracellular Mmp1 (green) relative to synaptic marker HRP (red) in control w^{1118}, $mmp2^{ss218/Df}$ and *UH1>Timp*. (B) Quantified fluorescent intensities normalized to controls (w^{1118}, *UH1*/+). (C) Extracellular Mmp2 (green) and HRP (red) in w^{1118}, $mmp1^{Q112*/Q273*}$ and *UH1>Timp*. (D) Quantified fluorescent intensities normalized to controls (w^{1118}, *UH1*/+). (E) Extracellular Timp (green) and HRP (red) in w^{1118} and $mmp2^{ss218/Df}$. Western blots of (F) Mmp1 (neuromusculature), (G) Mmp2 (whole tissue) and (H) Timp (neuromusculature). Genotypes: $mmp1^{Q112*/Q273*}$ (F-H), $mmp2^{W307*}$ and $mmp2^{W621*}$ (G) and $mmp2^{ss218/Df}$ (H). Further antibody characterization in Figs S6-S8. See Table S3 for raw data values and sample sizes. *P<0.05, ***P<0.001.

NMJs (Fig. 4C,D; Table S3A). Local Timp levels within the HRP-labeled NMJ terminal were unchanged in both *mmp1* and *mmp2* mutants, but the perisynaptic spatial domain of Timp expression was dramatically increased at *mmp2* LOF synapses (Fig. 4E, Table S3B). These immunocytochemistry results suggest that Mmp1 positively regulates Mmp2 levels, whereas Mmp2 negatively regulates both Mmp1 levels and localization of Timp.

To test whether changes were locally restricted or ubiquitous, we performed western blots on neuromusculature lysates. In agreement with imaging results, Mmp1 levels were increased in *mmp2* LOF lysates (Fig. 4F). By contrast, Mmp1 levels were strongly increased in *UH1>Timp* neuromusculature and in whole larvae (Fig. 4F, Fig. S6A). These differences may be due to Timp binding the Mmp1 catalytic domain to sterically hinder antibody accessibility (Fig. 4F, Fig. S6A). Mmp2 levels were also not noticeably decreased in *mmp1* LOF lysates, suggesting that these changes are locally restricted to the NMJ synapse (Fig. 4G). Similar to tissue immunocytochemistry results, Timp levels were comparable between mutants and controls (Fig. 4H). Taken together, these results reveal strong cross-talk between Mmp1, Mmp2 and Timp at the NMJ synapse, raising the possibility that tripartite complex interactions could contribute, at least in part, to the observed suppression mechanism.

Mmp1 and Mmp2 restrict Wnt trans-synaptic signaling

Extracellular regulation of trans-synaptic signaling is important for modulating both structural and functional synaptic development (Dani and Broadie, 2012; Parkinson et al., 2013; Dani et al., 2014). Both Mmp classes reside within the synaptomatrix, where they are perfectly positioned to participate in this mechanism and the LOF phenotypes are consistent with increased Wnt trans-synaptic signaling at the NMJ. Wnt signaling driving NMJ growth and synapse assembly involves the Wg ligand, HSPG co-receptor Dlp and Frizzled2 (Frz2) receptor (Friedman et al., 2013; Packard et al., 2002). In the Frizzled nuclear import (FNI) pathway, Frz2 is endocytosed following Wg activation, cleaved, transported into the muscle nuclei, where it associates with RNP granules containing synaptic transcripts and thereby drives expression changes modulating synapse structure and function (Mathew et al., 2005; Speese et al., 2012). This pathway is specifically misregulated in the *Drosophila* FXS disease model (Friedman et al., 2013) and associated NMJ synaptogenic phenotypes are remediated by either

Development (2016) 143, 75-87 doi:10.1242/dev.124461

genetic or pharmacological inhibition of Mmp (Siller and Broadie, 2011). Therefore, we tested whether this well-characterized Wnt mechanism is impacted by removal of Mmp.

At wild-type NMJs, the extracellular Wg ligand was localized to a dynamic subset of synaptic boutons (Fig. 5A). In *mmp1* LOF mutants, overall Wg levels at the NMJ were significantly decreased by ~40% (Fig. 5A,C, Table S3C). Because Mmps can facilitate signal localization, we assayed whether the percentage of Wg-expressing boutons was altered at *mmp1* mutant NMJs. Consistent with total abundance of Wg, *mmp1* mutants showed ~50% reduction in Wg-expressing boutons compared with matched controls (Fig. 5C, Table S3C). These results were replicated by *UH1>mmp1*^{RNAi}, but there were no significant changes in either *mmp2* LOF mutants or *UH1>mmp1+2*^{RNAi} animals (Fig. 5A,C, Table S3C). However, trans-synaptic FNI signal transduction via Frz2 receptor cleavage and FrzC2 intracellular trafficking to the muscle nuclei was increased in both Mmp single mutants. Importantly, this defect was not apparent in the *UH1>mmp1+2*^{RNAi} condition (Fig. 5B,D, Table S3C). It seems counter-intuitive that Wg was decreased in *mmp1* mutants alone, although both *mmp1* and *mmp2* mutants showed increased Wg signal transduction (FNI), yet there are multiple precedents for this observation at the *Drosophila* NMJ (Dani and Broadie, 2012; Friedman et al., 2013). Negative feedback is one possibility. In any case, the data are consistent with previous work showing that elevated Wg trans-synaptic signaling induces synaptic bouton formation (as in *mmp1* and *mmp2* mutants) and increases mEJC frequency (as in *mmp2* mutants) (Ataman et al., 2008), strongly reminiscent of the respective Mmp mutant phenotypes (Fig. 1, Fig. S2).

A recent report has shown that *Drosophila* Mmp2 directly cleaves the Wg HSPG co-receptor Dlp, in a mechanism that spatially tunes Wg signaling in developing ovary stem cells (Wang and Page-McCaw, 2014). This function provides a putative mechanism for Mmp misregulation of Wg trans-synaptic signaling during NMJ synaptogenesis, because Dlp is also an established Wg co-receptor and potent regulator of intercellular signaling at the developing synapse (Dani et al., 2012; Friedman et al., 2013; Johnson et al., 2006). Consistent with this hypothesis, Dlp was strongly reduced in *mmp1* LOF mutants (Fig. 6A, Table S3C). Moreover, there was also a strong defect in synaptic Dlp spatial distribution in both Mmp LOF mutants (Fig. 6B), which is consistent with known roles of Mmp in spatially regulating target proteins (Wang and Page-McCaw, 2014; Wang et al., 2010). First, a line scan through single synaptic boutons, with the intensity profile of Dlp (green) compared with the synaptic membrane marker HRP (red in Fig. 6B,C), showed that Dlp and HRP signals largely overlap in genetic controls, with a slight extension of Dlp beyond the HRP-marked membrane (Fig. 6C, left). By contrast, *mmp1* mutants showed strong reduction of the Dlp

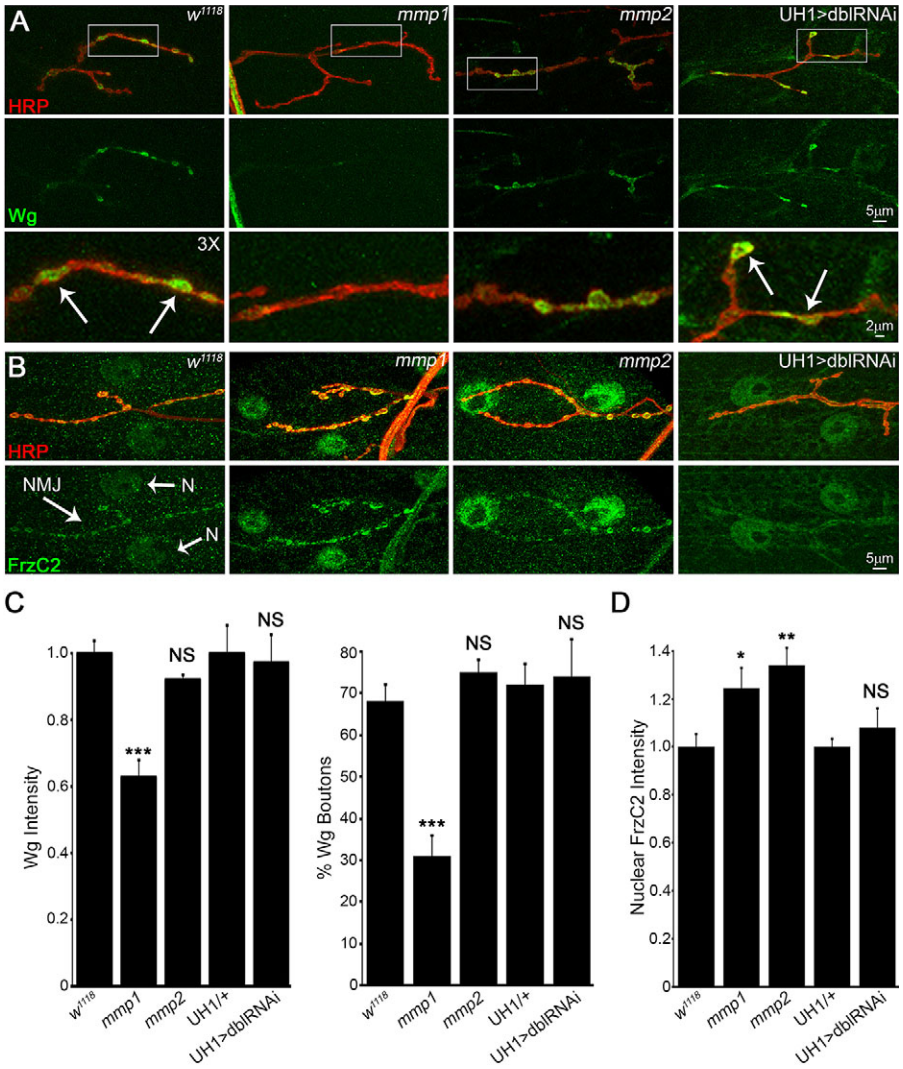

Fig. 5. Mmp1 and Mmp2 restrict Wnt trans-synaptic signal transduction. (A) NMJs labeled for extracellular Wg ligand (green) relative to synaptic HRP (red) in control (w^{1118}), *mmp1*$^{Q112*/Q273*}$, *mmp2*$^{ss218/Df}$ and *UH1>mmp1+2*^{RNAi} (dblRNAi). White boxes are enlarged 3× in bottom panels. Arrows indicate Wg-expressing boutons. (B) NMJs labeled for Frizzled 2 receptor C-terminus (Fz2-C, green) and HRP (red) in the same genotypes. Synaptic terminal (NMJ, arrow) and muscle nuclei (N, arrows) labeled in control. (C) Quantified Wg intensity (left) and percentage of Wg-expressing boutons (right) within HRP synaptic domain. (D) Quantified nuclear Fz2-C intensity in above genotypes. See Table S3C for raw data values and sample sizes. *P<0.05, **P<0.01, ***P<0.001; NS, not significant.

Development (2016) 143, 75-87 doi:10.1242/dev.124461

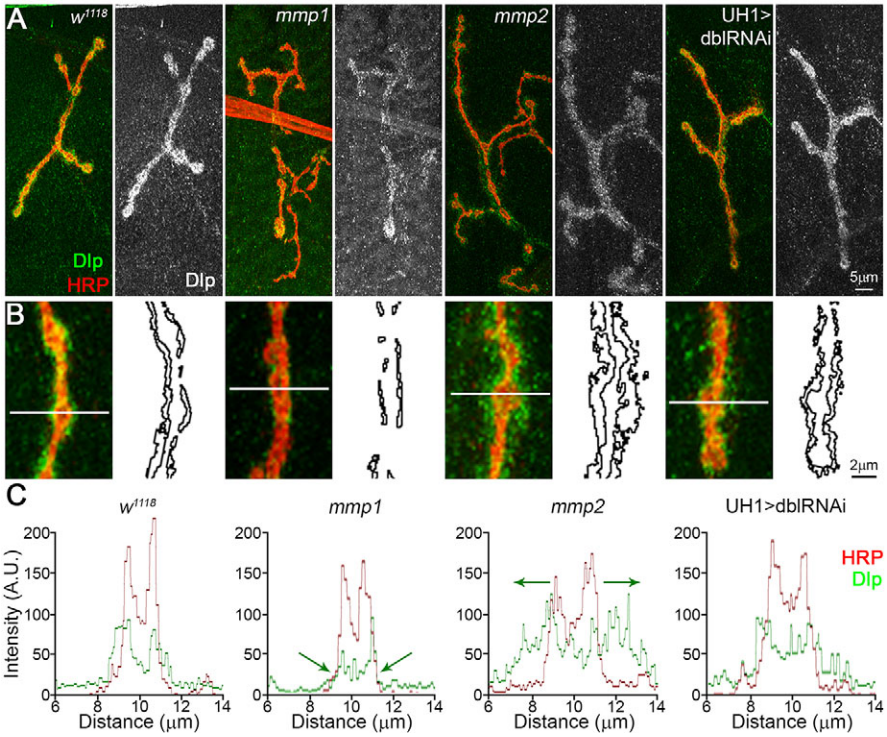

Fig. 6. Mmp1 and Mmp2 reciprocally regulate Wnt HSPG co-receptor Dlp. (A) NMJs labeled for Dlp (green) and HRP synaptic marker (red) in w^{1118}, $mmp1^{Q112*/Q273*}$, $mmp2^{ss218/Df}$ and *UH1>mmp1+2*^{RNAi} (dblRNAi). Black and white images show Dlp. (B) Higher magnification images of Dlp (green) at synaptic boutons (red). Skeleton outlines of Dlp area beyond HRP-masked NMJ are shown at the right. (C) Line-scan (line in panel B) of Dlp spatial expression (green) relative to HRP synaptic membrane marker (red). Arrows indicate Dlp spatial restriction in *mmp1* and expansion in *mmp2* mutants. See Table S3C for raw data values and sample sizes.

domain and *mmp2* LOF mutants showed strongly expanded Dlp domain (Fig. 6C, green arrows). Second, Dlp area outside the HRP-marked synaptic domain, normalized to NMJ area to account for terminal size, also showed that the spatial distribution of Dlp was reciprocally regulated by Mmp1 and Mmp2. Dlp area decreased ~40% in *mmp1* LOF mutants and increased almost twofold in *mmp2* LOF mutants (Fig. 6, Table S3C). Importantly, Dlp spatial misregulation was not detected in the *UH1>mmp1+2*^{RNAi} condition (Fig. 6, Table S3C).

Restoring Wnt co-receptor Dlp levels in Mmp mutants prevents synaptogenic defects

Our working model proposes that the two Mmp classes, balanced by Timp inhibition and reciprocal co-suppression, mediate synaptomatrix control of Wnt trans-synaptic signaling at the level of the Dlp co-receptor to coordinate structural and functional development of the NMJ. If this hypothesis is correct, the altered Dlp levels and/or spatial distribution should be causative for the synaptogenic defects in both classes of Mmp mutants. To test this prediction, we created lines to compensate for changes in Dlp levels in each Mmp mutant, and then tested for correction of both structural and functional defects (Fig. 7, Tables S1A, S2A, 'Dlp modulation'). In *mmp1* LOF mutants, Dlp was significantly reduced in the postsynaptic compartment and therefore, we transgenically increased Dlp expression in the muscle ($mmp1^{Q112*/Q273*}$; *24B>UAS-dlp*). Conversely, in *mmp2* mutants, Dlp was spatially expanded and therefore, we removed one *dlp* gene copy to reduce levels ($mmp2^{W307*/Df}$; $dlp^{A187/+}$). In both *mmp1* and *mmp2* mutants, correcting Dlp expression toward normal levels suppressed the synaptic morphogenesis defects (Fig. 7A, Table S1A). Quantification of the number of synaptic boutons showed that *mmp1* supernumerary boutons were completely prevented by elevated levels of postsynaptic Dlp (Fig. 7B). Likewise, the elevated number of synaptic boutons in *mmp2* mutants was completely prevented by reducing Dlp levels with the *dlp*/+ heterozygote (Fig. 7B). Next, EJC recordings to assay neurotransmission strength in both *mmp1* and *mmp2* mutants showed that correcting Dlp levels reduced the elevated transmission in both cases (Fig. 7C, Table S2A). Quantification of EJC amplitude showed that postsynaptic Dlp expression in *mmp1* mutants prevented the elevated transmission and reversed the phenotype to cause significantly reduced transmission (Fig. 7D). In *mmp2* mutants, reduction of the Dlp levels restored EJC amplitude towards the control level, showing a significant reduction from the mutant level, with no significant difference remaining compared with the control (Fig. 7D). Thus, both increased NMJ structural development and elevated neurotransmission strength in both classes of Mmp mutant were rectified by manipulating Dlp expression back towards wild-type levels.

DISCUSSION

A large number of Mmps are expressed in the mammalian nervous system, with roles in neurodevelopment, plasticity and neurological disease (Fujioka et al., 2012). Understanding how each Mmp individually and combinatorially functions is hindered by genetic redundancy and compensatory mechanisms. We have therefore exploited the *Drosophila* system to analyze a matrix metalloproteome containing just one member of each conserved component: one secreted Mmp, one membrane-tethered Mmp and one Timp (Glasheen et al., 2009; Page-McCaw et al., 2003, 2007). We found that both Mmp classes attenuate structural and functional synaptic development, with electrophysiological, ultrastructural and molecular roles in both presynaptic and postsynaptic cells. A surprising discovery is that the Mmp classes suppress each other's requirements at the synapse. From discrete activities to redundancy, cooperation and now reciprocal suppression, studies continue to reveal how Mmps interact to regulate developmental processes (Jia et al., 2014; Miller et al., 2008; Wang and Page-McCaw, 2014). This study shows that the two Mmp classes play separable yet interactive roles in sculpting

Development (2016) 143, 75-87 doi:10.1242/dev.124461

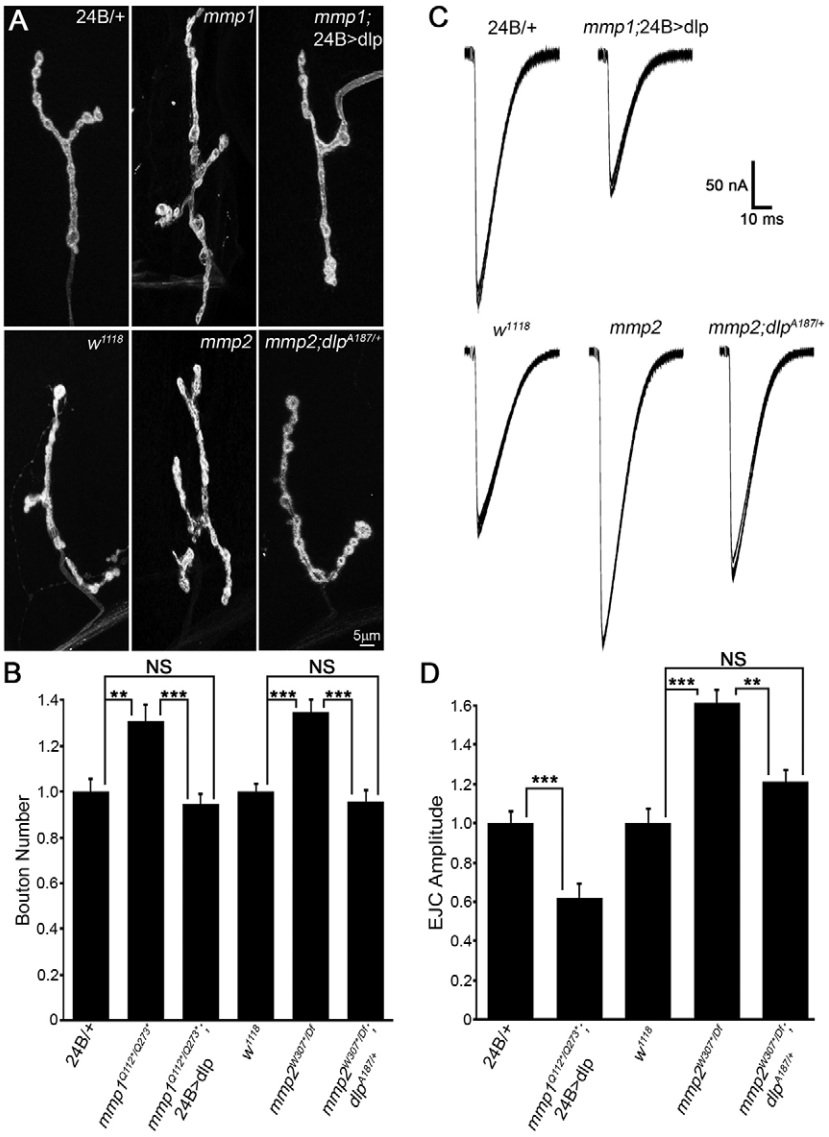

Fig. 7. Restoring Dlp levels in Mmp mutants prevents defects in NMJ structure or function. (A) NMJs labeled for HRP and Dlg. Top row: *24B/+* transgenic control, *mmp1*$^{Q112*/Q273*}$ and *mmp1*$^{Q112*/Q273*}$; *24B>UAS-dlp*. Bottom row: *w*^{1118} genetic control, *mmp2*$^{W307*/Df}$ and *mmp2*$^{W307*/Df}$; *dlp*$^{A187/+}$. (B) Quantified bouton number normalized to controls for above genotypes. (C) EJC traces recorded from denoted genotypes. Top row: *24B/+* transgenic control (left) and *mmp1*$^{Q112*/Q273*}$; *24B>UAS-dlp* (right). Bottom row: *w*^{1118} genetic control, *mmp2*$^{W307*/Df}$ and *mmp2*$^{W307*/Df}$; *dlp*$^{A187/+}$. (D) Quantified EJC amplitudes normalized to controls for above genotypes. See Table S1A for raw data values and sample sizes. $^{**}P<0.01$, $^{***}P<0.001$; NS, not significant.

NMJ development. During the writing of this manuscript, a genomic Mmp2 rescue line was produced (Wang and Page-McCaw, 2014), which will be critical in further testing this interactive mechanism. It will be interesting to determine whether the Mmp suppressive mechanism is used in other developmental contexts, other intercellular signaling pathways and in mammalian models. Mammalian Mmp9 regulates synapse architecture and also postsynaptic glutamate receptor expression and/or localization (Dziembowska and Wlodarczyk, 2012; Michaluk et al., 2009; Wilczynski et al., 2008). Likewise, mammalian Mmp7 regulates both presynaptic properties and postsynaptic glutamate receptor subunits (Szklarczyk et al., 2007, 2008). Thus, the dual roles of Mmps in pre- and postsynaptic compartments appear to be evolutionarily conserved.

Previous work demonstrated that Mmp1 and Mmp2 both regulate motor axon pathfinding in *Drosophila* embryos, albeit to different degrees and here, double Mmp mutants still exhibited defasciculated nerve bundles that separate prematurely (Miller et al., 2008). Consistently, both Mmp single mutants display excessive terminal axon branching at the postembryonic NMJ, but here the defect is fully alleviated by the removal of both Mmps. To our knowledge, other studies have either not identified, or not tested, a similar Mmp interaction, suggesting that reciprocal suppression might be specific to synaptogenesis. However, there are numerous reports that highlight the importance of Mmp and Timp balance. Mmp:Timp ratios can influence protease activation, localization, substrate specificity and Timp signaling and are commonly used as predictive clinical correlates in disease pathology (Moore and Crocker, 2012; Nagase et al., 2006; Romi et al., 2012). At the *Drosophila* NMJ, a similar reciprocal suppression interaction between *pgant* glycosyltransferases involved in *O*-linked glycosylation regulates synaptogenesis via integrin-tenascin trans-synaptic signaling (Dani et al., 2014). A recent study reported that *pgant* activity protects substrates from Furin-mediated proteolysis, which is a protease responsible for processing or activating *Drosophila* Mmp1 and Mmp2 (Zhang et al., 2014). Thus, Mmp proteolytic and glycan mechanisms could converge within the NMJ synaptomatrix to regulate trans-synaptic signaling.

New antibody tools produced here provide the means to interrogate an entire matrix metalloproteome, and will be important for testing Mmp and Timp functions throughout *Drosophila*. Many Mmps are both developmentally and activity regulated, with highly context-dependent functions (Benson and Huntley, 2012; Dziembowska and Wlodarczyk, 2012; Ethell and

Development (2016) 143, 75-87 doi:10.1242/dev.124461

Ethell, 2007). Our future work will temporally dissect this mechanism at the developing NMJ and investigate how activity might regulate Mmp localization and function. It will be informative to correlate synaptogenic Mmp requirements with Mmp enzymatic activity by using *in situ* zymography assays, although non-enzymatic roles are certainly also possible. Lack of ultrastructure defects in Mmp mutant NMJs suggests that *Drosophila* Mmps have primarily instructive functions at the synapse, rather than broad proteolytic roles in ECM degradation. Consistently, *Drosophila* Mmp2 instructs motor axon pathfinding via a BMP intercellular signaling mechanism (Miller et al., 2011). Conversely, Mmp2 functions permissively in basement membrane degradation while shaping dendritic arbors (Yasunaga et al., 2010). Because synaptic bouton size is reduced in *mmp1* mutants, Mmp1 activity might degrade a prohibitive physical barrier at the NMJ. However, our results indicate a primary Mmp role in regulating intercellular signaling during synaptic development.

HSPG co-receptors of trans-synaptic ligands are key modulators of NMJ synaptogenesis (Dani et al., 2012; Friedman et al., 2013; Johnson et al., 2006; Kamimura et al., 2013) and HSPGs are also established substrates of both mammalian and *Drosophila* Mmps (Kessenbrock et al., 2010; Wang and Page-McCaw, 2014). Mmp1 and Mmp2 differentially regulate the HSPG Dlp co-receptor to restrict the Wnt Wg trans-synaptic signaling driving structural and functional NMJ development (Mathew et al., 2005; Packard et al., 2002; Speese et al., 2012). How might both increased and decreased levels of the Dlp co-receptor yield increased FNI pathway signal transduction? Regulation of Wnt signaling interactions ligands, co-receptors and receptors is managed at many levels (van Amerongen, 2012). The 'Wg exchange factor model' (Yan et al., 2009) provides a mechanistic framework for understanding the suppressive interactions of Mmp. In this mechanism, a low Dlp:Frz2 ratio helps the Frz2 receptor obtain more Wg, whereas a high Dlp:Frz2 ratio prevents Frz2 from capturing Wg as Dlp competes and sequesters Wg away from Frz2. Importantly, however, Dlp exhibits a context-dependent, bimodal role as both activator and repressor (Wu et al., 2010). Indeed, our previous studies show these mechanisms are a key driving force in Wg signal transduction at the *Drosophila* NMJ (Dani et al., 2012; Friedman et al., 2013). In *mmp1* mutants, Wg and Dlp are both reduced, resulting in a low Dlp:Frz2 ratio and elevated FNI. In *mmp2* mutants, Dlp is spatially diffuse and Frz2 is increased, similarly resulting in a low Dlp:Frz2 ratio and elevated FNI. Balance is reset with Mmp co-removal because neither form of Mmp-induced HSPG tuning occurs. In this regard, it might be predicted that Dlp reduction in *mmp2* mutants would only further increase FNI and therefore structural and functional defects. However, $mmp2^{W307*/Df}$;$dlp^{A187/+}$ NMJs are indistinguishable from controls. It is therefore likely that absolute Dlp levels are the important driving factor in synaptogenesis and/or that Dlp exhibits bimodal functions in synaptic development.

Interestingly, a recent mouse study showed the Mmp3 hemopexin domain promotes Wnt signaling by inhibiting a negative Wnt regulator, raising the possibility that Mmps can act as molecular switches (or in feedback loops) dictating Wnt transduction (Kessenbrock et al., 2013). Another study suggests that Wnt signaling can directly mediate co-regulation of heparanase and Mmps (Zcharia et al., 2009). Indeed, both neural activity and intercellular signaling can stimulate Mmp-dependent ectodomain shedding of plasma membrane target proteins, thereby directly regulating the surface abundance of HSPGs and receptors, as well as other Mmps, which thus reciprocally modulate intra- and extracellular organization (Dansie and Ethell, 2011; Huntley, 2012; Tian et al., 2007). From this model, the spatial arrangement of Dlp could be affected by co-regulated sheddase activity that is differentially altered in *mmp1* and *mmp2* mutants. Specifically, Mmp2 could shed Dlp, resulting in an increased area of Dlp expression in *mmp2* mutants and loss of Mmp2 regulation by Mmp1 could result in aberrant Dlp restriction in *mmp1* mutants, with Mmp co-removal remediating the Dlp domain thereby restoring normal Wnt trans-synaptic signaling. Our future work will test the reciprocal impacts of Wnt signaling on Mmp expression and/or function in the context of synaptic development.

Emerging evidence suggests HSPG glycosaminoglycan (GAG) chains function as allosteric regulators of Mmps, with GAG content or composition influencing the localization and substrate specificity of Mmp (Tocchi and Parks, 2013). Indeed, studies from our lab and others show that Wg signaling is sensitive to perturbations in HSPG chain biosynthesis and HS modifying enzymes, which modulate both NMJ structure and function (Dani et al., 2012; Menon et al., 2013; Reichsman et al., 1996; Ren et al., 2009). It is easy to envision how tissue- and development-stage-specific HS modifications could coordinate HSPG/Mmp-dependent functions, thereby differentially regulating diverse signaling events, which enable context-specific responses instructed by the extracellular environment. Future work will examine how dual inputs of the HSPG co-receptor function and how Mmp proteolytic cleavage coordinates Wnt trans-synaptic signaling during synaptogenesis, particularly in the context of our Fragile X syndrome (FXS) disease model (Coffee et al., 2010; Tessier and Broadie, 2012). Given that both loss or inhibition Mmp (Siller and Broadie, 2011) and correction of HSPG elevation (Friedman et al., 2013) independently alleviate synaptic defects in the FXS disease state, the overlapping mechanism provides an exciting avenue to therapeutic interventions for FXS and, potentially, related intellectual disability and autism spectrum disorders.

MATERIALS AND METHODS

Drosophila stocks

All strains were maintained on standard medium at 25°C. The Mmp mutants used included: point mutant null $mmp1^{Q112*}$, P-element deletion null $mmp1^{2}$ and point mutant hypomorph $mmp1^{Q273*}$; point mutant null $mmp2^{W307*}$, deficiency null $mmp2^{Df(2R)Uba1\text{-}Mmp2}$, point mutant hypomorph $mmp2^{W621*}$ and 3′ splice-site genetic-null $mmp2^{ss218}$ (Jia et al., 2014; Page-McCaw et al., 2003). The double heterozygous (dblhet) genotype was $mmp1^{Q112*/+}$; $mmp2^{W307*/+}$. The *timp*-null deficiency was $timp^{1}syn^{28}$ (Godenschwege et al., 2000). Knockdown studies used UAS-$mmp1^{RNAi}$, UAS-$mmp2^{RNAi}$ (Uhlirova and Bohmann, 2006) and UAS-$mmp2^{dsRNAi1794\text{-}1R\text{-}2}$ (NIG-Fly). Pan-neuronal *elav-Gal4*, motoneuron-specific *D42-Gal4*, pan-muscle *24B-Gal4* and ubiquitous *UH1-Gal4* drivers were obtained from the Bloomington *Drosophila* Stock Center (Indiana University). *24B-Gal4* and *elav-Gal4* were recombined in a dual driver line. Double inhibition studies included *UAS-timp* (Page-McCaw et al., 2003) overexpression (OE) and double *UAS-*$mmp1^{RNAi}$; *UAS-*$mmp2^{dsRNAi1794\text{-}1R\text{-}2}$ (dblRNAi). *UAS-dlp* (Baeg et al., 2001) and dlp^{A187} deletion (Han et al., 2004) were used in Dlp modulation studies. Genetic controls included w^{1118} and Gal4 drivers crossed into the w^{1118} background.

Antibody production and western blot analyses

Constructs for Mmp2 and Timp were optimized and ordered from GenArt. His-tagged Mmp2 and MBP-tagged Timp proteins were recombinantly expressed in *E. coli* and purified in the Vanderbilt Antibody and Protein Resource core (VAPR). See supplementary Materials and Methods for full sequences. SDS-PAGE western blots of neuromusculature and CNS were performed as previously described (Parkinson et al., 2013). For further

Development (2016) 143, 75-87 doi:10.1242/dev.124461

details of methods and antibodies used for blotting, see supplementary Materials and Methods.

Immunocytochemistry imaging

Larval NMJ preparations were processed with (permeabilized) or without (extracellular labeling) detergent, incubated overnight in primary antibodies, including; mouse anti-Mmp1 (1:10; DSHB), rabbit anti-Mmp2 (1:1000; this study), rabbit anti-Timp (1:500; this study), rabbit anti-HRP (1:200; Sigma, P7899), goat anti-HRP (1:200; Jackson Laboratories, 123-165-021), mouse anti-Dlg (1:200; DSHB), mouse anti-GluRIIA (1:100; DHSB), rabbit anti-GluRIIB (1:1000, Chen and Featherstone, 2005), rabbit anti-GluRIID (1:500; Chen and Featherstone, 2005), mouse anti-BRP (1:100; DHSB), mouse anti-Wg (1:2; DSHB), rabbit anti-DFz2-C (1:500; Mathew et al., 2005) and mouse anti-Dlp (1:5; DSHB). For details of all secondary antibodies used, see supplementary Materials and Methods.

Electrophysiology

Two-electrode voltage-clamp (TEVC) records were made in 128 mM NaCl, 2 mM KCl, 4 mM $MgCl_2$, 1.0 mM $CaCl_2$, 70 mM sucrose and 5 mM HEPES at pH 7.1. Recording electrodes of >15 MΩ (1 mm outer diameter; World Precision Instruments) were used to record from muscle six voltage-clamped (V_{hold}, −60 mV) with an Axoclamp2B amplifier (Molecular Devices) in the episodic recording configuration. Evoked EJC records were made with nerve stimulation using glass suction electrodes at supra-threshold voltages (50% above threshold) for 0.5 ms at 0.2 Hz. Spontaneous mEJC records were obtained following cutting of the segmental nerves. Records were acquired with Clampex (Molecular Devices) and analyzed using Clampfit 9.0.

Electron microscopy

Larvae were dissected and fixed in 4% PFA+0.1% glutaraldehyde for 1 h, then post-fixed in 1% osmium tetroxide for 1 h. Preparations were dehydrated in an ethanol, propylene oxide and resin infiltration series. Muscle 6/7 was dissected free and placed in a resin block. Ultrathin (40 nm) sections were made (Leica Ultracut UCT ultramicrotome), collected on Formvar-coated grids, and imaged using a Phillips CM10 transmission electron microscope at 80 kV. Imaging was done with a 4 megapixel AMT CCD camera. Bouton area was defined by the greatest cross-sectional area containing an electron-dense T-bar active zone.

Statistical measurements

All analyses were done on stage- or size-matched animals. All images were projected in Zeiss LSM Image Examiner. Type IB synaptic boutons were defined as HRP- and Dlg-positive varicosities ≥2 µm in diameter (Gatto and Broadie, 2008). Bouton volume was determined using the Volumest plugin in ImageJ (Doll and Broadie, 2015). Intensity measurements were made with HRP signal delineated *z*-stack areas of maximum projection. Dlp area measurements were quantified as fluorescent signal area normalized to HRP area calculated in ImageJ. The Zeiss LSM line profile function was used for line scan quantification through boutons. GluR and Brp puncta measurements were normalized to bouton volume for five boutons per NMJ. Images for display were exported to Adobe Photoshop. Data presented as means±s.e.m. Statistical comparisons were performed using Instat3 software (GraphPad Software). Mann–Whitney *U*-tests were used for nonparametric comparisons. ANOVA tests were used for data sets of ≥3 comparisons followed by appropriate post-hoc analyses. Raw data values and sample sizes are listed in Tables S1-S3.

Acknowledgements

We thank the Bloomington *Drosophila* Stock Center (Indiana University) and Developmental Studies Hybridoma Bank (DSHB, University of Iowa) for providing key resources for this study. We thank Andrea Page-McCaw (Vanderbilt University) and Sheng Li (Shanghai Institute for Biological Sciences) for Mmp mutants, Patricia Jumbo-Lucioni (Broadie Lab) for the recombined *elav-Gal4*, *24B-Gal4* driver and Emma Rushton (Broadie Lab) for help with genetics. Antibody gifts included DFz2-C from Vivian Budnik (University of Massachusetts Medical School), GluRIID from Stephan Sigrist (Institute of Biology, FU Berlin, Germany), and GluRIIB from Aaron DiAntonio (Washington University) and David Featherstone (University of Illinois, Chicago). We thank the Vanderbilt Antibody and Protein Resource (VAPR) core for help making Mmp2 and Timp antibodies.

Competing interests

The authors declare no competing or financial interests.

Author contributions

M.L.D. and S.Z. performed all confocal imaging and western blot experiments. N.D. performed electrophysiology experiments. W.P. performed electron microscopy experiments. K.B. designed all experiments and oversaw all studies. The manuscript was co-written by M.L.D. and K.B.

Funding

This work was supported by the National Institutes of Health [MH096832 to K.B.]. Deposited in PMC for release after 12 months.

Supplementary information

Supplementary information available online at
http://dev.biologists.org/lookup/suppl/doi:10.1242/dev.124461/-/DC1

References

Agrawal, S. M., Lau, L. and Yong, V. W. (2008). MMPs in the central nervous system: where the good guys go bad. *Semin. Cell Dev. Biol.* **19**, 42-51.

Ataman, B., Ashley, J., Gorczyca, M., Ramachandran, P., Fouquet, W., Sigrist, S. J. and Budnik, V. (2008). Rapid activity-dependent modifications in synaptic structure and function require bidirectional Wnt signaling. *Neuron* **57**, 705-718.

Baeg, G. H., Lin, X. H., Khare, N., Baumgartner, S. and Perrimon, N. (2001). Heparan sulfate proteoglycans are critical for the organization of the extracellular distribution of Wingless. *Development* **128**, 87-94.

Benson, D. L. and Huntley, G. W. (2012). Building and remodeling synapses. *Hippocampus* **22**, 954-968.

Bilousova, T. V., Dansie, L., Ngo, M., Aye, J., Charles, J. R., Ethell, D. W. and Ethell, I. M. (2009). Minocycline promotes dendritic spine maturation and improves behavioural performance in the fragile X mouse model. *J. Med. Genet.* **46**, 94-102.

Chen, K. and Featherstone, D. E. (2005). Discs-large (DLG) is clustered by presynaptic innervation and regulates postsynaptic glutamate receptor subunit composition in Drosophila. *BMC Biol.* **3**, 1.

Coffee, R. L., Tessier, C. R., Woodruff, E. A. and Broadie, K. (2010). Fragile X mental retardation protein has a unique, evolutionarily conserved neuronal function not shared with FXR1P or FXR2P. *Dis. Model. Mech.* **3**, 471-485.

Dani, N. and Broadie, K. (2012). Glycosylated synaptomatrix regulation of trans-synaptic signaling. *Dev. Neurobiol.* **72**, 2-21.

Dani, N., Nahm, M., Lee, S. and Broadie, K. (2012). A targeted glycan-related gene screen reveals heparan sulfate proteoglycan sulfation regulates WNT and BMP trans-synaptic signaling. *PLoS Genet.* **8**, e1003031.

Dani, N., Zhu, H. and Broadie, K. (2014). Two protein N-acetylgalactosaminyl transferases regulate synaptic plasticity by activity-dependent regulation of integrin signaling. *J. Neurosci.* **34**, 13047-13065.

Dansie, L. E. and Ethell, I. M. (2011). Casting a net on dendritic spines: the extracellular matrix and its receptors. *Dev. Neurobiol.* **71**, 956-981.

Davis, G. W. and Müller, M. (2015). Homeostatic control of presynaptic neurotransmitter release. *Annu. Rev. Physiol.* **77**, 251-270.

Diantonio, A., Petersen, S. A., Heckmann, M. and Goodman, C. S. (1999). Glutamate receptor expression regulates quantal size and quantal content at the Drosophila neuromuscular junction. *J. Neurosci.* **19**, 3023-3032.

Doll, C. A. and Broadie, K. (2014). Impaired activity-dependent neural circuit assembly and refinement in autism spectrum disorder genetic models. *Front. Cell. Neurosci.* **8**, 30.

Doll, C. A. and Broadie, K. (2015). Activity-dependent FMRP requirements in development of the neural circuitry of learning and memory. *Development* **142**, 1346-1356.

Dziembowska, M. and Wlodarczyk, J. (2012). MMP9: a novel function in synaptic plasticity. *Int. J. Biochem. Cell Biol.* **44**, 709-713.

Ethell, I. M. and Ethell, D. W. (2007). Matrix metalloproteinases in brain development and remodeling: synaptic functions and targets. *J. Neurosci. Res.* **85**, 2813-2823.

Friedman, S. H., Dani, N., Rushton, E. and Broadie, K. (2013). Fragile X mental retardation protein regulates trans-synaptic signaling in Drosophila. *Dis. Model. Mech.* **6**, 1400-1413.

Fujioka, H., Dairyo, Y., Yasunaga, K.-I. and Emoto, K. (2012). Neural functions of matrix metalloproteinases: plasticity, neurogenesis, and disease. *Biochem. Res. Int.* **2012**, 789083.

Gatto, C. L. and Broadie, K. (2008). Temporal requirements of the fragile X mental retardation protein in the regulation of synaptic structure. *Development* **135**, 2637-2648.

Gatto, C. L. and Broadie, K. (2011). Drosophila modeling of heritable neurodevelopmental disorders. *Curr. Opin. Neurobiol.* **21**, 834-841.
Glasheen, B. M., Kabra, A. T. and Page-McCaw, A. (2009). Distinct functions for the catalytic and hemopexin domains of a Drosophila matrix metalloproteinase. *Proc. Natl. Acad. Sci. USA* **106**, 2659-2664.
Godenschwege, T. A., Pohar, N., Buchner, S. and Buchner, E. (2000). Inflated wings, tissue autolysis and early death in tissue inhibitor of metalloproteinases mutants of Drosophila. *Eur. J. Cell Biol.* **79**, 495-501.
Han, C., Belenkaya, T. Y., Wang, B. and Lin, X. (2004). Drosophila glypicans control the cell-to-cell movement of Hedgehog by a dynamin-independent process. *Development* **131**, 601-611.
Huntley, G. W. (2012). Synaptic circuit remodelling by matrix metalloproteinases in health and disease. *Nat. Rev. Neurosci.* **13**, 743-757.
Jia, Q., Liu, Y., Liu, H. and Li, S. (2014). Mmp1 and Mmp2 cooperatively induce Drosophila fat body cell dissociation with distinct roles. *Sci. Rep.* **4**, 7535.
Johnson, K. G., Tenney, A. P., Ghose, A., Duckworth, A. M., Higashi, M. E., Parfitt, K., Marcu, O., Heslip, T. R., Marsh, J. L., Schwarz, T. L. et al. (2006). The HSPGs syndecan and dallylike bind the receptor phosphatase LAR and exert distinct effects on synaptic development. *Neuron* **49**, 517-531.
Kamimura, K., Ueno, K., Nakagawa, J., Hamada, R., Saitoe, M. and Maeda, N. (2013). Perlecan regulates bidirectional Wnt signaling at the Drosophila neuromuscular junction. *J. Cell Biol.* **200**, 219-233.
Kessenbrock, K., Plaks, V. and Werb, Z. (2010). Matrix metalloproteinases: regulators of the tumor microenvironment. *Cell* **141**, 52-67.
Kessenbrock, K., Dijkgraaf, G. J. P., Lawson, D. A., Littlepage, L. E., Shahi, P., Pieper, U. and Werb, Z. (2013). A role for matrix metalloproteinases in regulating mammary stem cell function via the Wnt signaling pathway. *Cell Stem Cell* **13**, 300-313.
Kuo, C. T., Jan, L. Y. and Jan, Y. N. (2005). Dendrite-specific remodeling of Drosophila sensory neurons requires matrix metalloproteases, ubiquitin-proteasome, and ecdysone signaling. *Proc. Natl. Acad. Sci. USA* **102**, 15230-15235.
Llano, E., Pendás, A. M., Aza-Blanc, P., Kornberg, T. B. and López-Otín, C. (2000). Dm1-MMP, a matrix metalloproteinase from Drosophila with a potential role in extracellular matrix remodeling during neural development. *J. Biol. Chem.* **275**, 35978-35985.
Llano, E., Adam, G., Pendás, A. M., Quesada, V., Sánchez, L. M., Santamariá, I., Noselli, S. and López-Otín, C. (2002). Structural and enzymatic characterization of Drosophila Dm2-MMP, a membrane-bound matrix metalloproteinase with tissue-specific expression. *J. Biol. Chem.* **277**, 23321-23329.
Long, A. A., Mahapatra, C. T., Woodruff, E. A., Rohrbough, J., Leung, H.-T., Shino, S., An, L., Doerge, R. W., Metzstein, M. M., Pak, W. L. et al. (2010). The nonsense-mediated decay pathway maintains synapse architecture and synaptic vesicle cycle efficacy. *J. Cell Sci.* **123**, 3303-3315.
Marrus, S. B. and DiAntonio, A. (2004). Preferential localization of glutamate receptors opposite sites of high presynaptic release. *Curr. Biol.* **14**, 924-931.
Mathew, D., Ataman, B., Chen, J., Zhang, Y., Cumberledge, S. and Budnik, V. (2005). Wingless signaling at synapses is through cleavage and nuclear import of receptor DFrizzled2. *Science* **310**, 1344-1347.
Menon, K. P., Carrillo, R. A. and Zinn, K. (2013). Development and plasticity of the Drosophila larval neuromuscular junction. *Wiley Interdiscip. Rev. Dev. Biol.* **2**, 647-670.
Michaluk, P., Mikasova, L., Groc, L., Frischknecht, R., Choquet, D. and Kaczmarek, L. (2009). Matrix metalloproteinase-9 controls NMDA receptor surface diffusion through integrin beta1 signaling. *J. Neurosci.* **29**, 6007-6012.
Miller, C. M., Page-McCaw, A. and Broihier, H. T. (2008). Matrix metalloproteinases promote motor axon fasciculation in the Drosophila embryo. *Development* **135**, 95-109.
Miller, C. M., Liu, N., Page-McCaw, A. and Broihier, H. T. (2011). Drosophila MMP2 regulates the matrix molecule faulty attraction (Frac) to promote motor axon targeting in Drosophila. *J. Neurosci.* **31**, 5335-5347.
Mohrmann, R., Matthies, H. J., Woodruff, E. and Broadie, K. (2008). Stoned B mediates sorting of integral synaptic vesicle proteins. *Neuroscience* **153**, 1048-1063.
Moore, C. S. and Crocker, S. J. (2012). An alternate perspective on the roles of TIMPs and MMPs in pathology. *Am. J. Pathol.* **180**, 12-16.
Nagase, H., Visse, R. and Murphy, G. (2006). Structure and function of matrix metalloproteinases and TIMPs. *Cardiovasc. Res.* **69**, 562-573.
Packard, M., Koo, E. S., Gorczyca, M., Sharpe, J., Cumberledge, S. and Budnik, V. (2002). The Drosophila Wnt, wingless, provides an essential signal for pre- and postsynaptic differentiation. *Cell* **111**, 319-330.
Page-McCaw, A., Serano, J., Sante, J. M. and Rubin, G. M. (2003). Drosophila matrix metalloproteinases are required for tissue remodeling, but not embryonic development. *Dev. Cell* **4**, 95-106.
Page-McCaw, A., Ewald, A. J. and Werb, Z. (2007). Matrix metalloproteinases and the regulation of tissue remodelling. *Nat. Rev. Mol. Cell Biol.* **8**, 221-233.
Parkinson, W., Dear, M. L., Rushton, E. and Broadie, K. (2013). N-glycosylation requirements in neuromuscular synaptogenesis. *Development* **140**, 4970-4981.
Pollock, E., Everest, M., Brown, A. and Poulter, M. O. (2014). Metalloproteinase inhibition prevents inhibitory synapse reorganization and seizure genesis. *Neurobiol. Dis.* **70**, 21-31.
Qin, G., Schwarz, T., Kittel, R. J., Schmid, A., Rasse, T. M., Kappei, D., Ponimaskin, E., Heckmann, M. and Sigrist, S. J. (2005). Four different subunits are essential for expressing the synaptic glutamate receptor at neuromuscular junctions of Drosophila. *J. Neurosci.* **25**, 3209-3218.
Reichsman, F., Smith, L. and Cumberledge, S. (1996). Glycosaminoglycans can modulate extracellular localization of the wingless protein and promote signal transduction. *J. Cell Biol.* **135**, 819-827.
Reinhard, S. M., Razak, K. and Ethell, I. M. (2015). A delicate balance: role of MMP-9 in brain development and pathophysiology of neurodevelopmental disorders. *Front. Cell. Neurosci.* **9**, 280.
Ren, Y., Kirkpatrick, C. A., Rawson, J. M., Sun, M. and Selleck, S. B. (2009). Cell type-specific requirements for heparan sulfate biosynthesis at the Drosophila neuromuscular junction: effects on synapse function, membrane trafficking, and mitochondrial localization. *J. Neurosci.* **29**, 8539-8550.
Rohrbough, J., Rushton, E., Woodruff, E., Fergestad, T., Vigneswaran, K. and Broadie, K. (2007). Presynaptic establishment of the synaptic cleft extracellular matrix is required for post-synaptic differentiation. *Genes Dev.* **21**, 2607-2628.
Romi, F., Helgeland, G. and Gilhus, N. E. (2012). Serum levels of matrix metalloproteinases: implications in clinical neurology. *Eur. Neurol.* **67**, 121-128.
Shinoe, T. and Goda, Y. (2015). Tuning synapses by proteolytic remodeling of the adhesive surface. *Curr. Opin. Neurobiol.* **35**, 148-155.
Sidhu, H., Dansie, L. E., Hickmott, P. W., Ethell, D. W. and Ethell, I. M. (2014). Genetic removal of matrix metalloproteinase 9 rescues the symptoms of fragile X syndrome in a mouse model. *J. Neurosci.* **34**, 9867-9879.
Siller, S. S. and Broadie, K. (2011). Neural circuit architecture defects in a Drosophila model of Fragile X syndrome are alleviated by minocycline treatment and genetic removal of matrix metalloproteinase. *Dis. Model. Mech.* **4**, 673-685.
Siller, S. S. and Broadie, K. (2012). Matrix metalloproteinases and minocycline: therapeutic avenues for fragile X syndrome. *Neural Plast.* **2012**, 124548.
Speese, S. D., Ashley, J., Jokhi, V., Nunnari, J., Barria, R., Li, Y., Ataman, B., Koon, A., Chang, Y.-T., Li, Q. et al. (2012). Nuclear envelope budding enables large ribonucleoprotein particle export during synaptic Wnt signaling. *Cell* **149**, 832-846.
Sternlicht, M. and Werb, Z. (2001). How matrix metalloproteinases regulate cell behavior. *Annu. Rev. Cell Biol.* **17**, 463-516.
Szklarczyk, A., Conant, K., Owens, D. F., Ravin, R., McKay, R. D. and Gerfen, C. (2007). Matrix metalloproteinase-7 modulates synaptic vesicle recycling and induces atrophy of neuronal synapses. *Neuroscience* **149**, 87-98.
Szklarczyk, A., Ewaleifoh, O., Beique, J.-C., Wang, Y., Knorr, D., Haughey, N., Malpica, T., Mattson, M. P., Huganir, R. and Conant, K. (2008). MMP-7 cleaves the NR1 NMDA receptor subunit and modifies NMDA receptor function. *FASEB J.* **22**, 3757-3767.
Tessier, C. R. and Broadie, K. (2012). Molecular and Genetic Analysis of the Drosophila Model of Fragile X Syndrome. In *Modeling Fragile X Syndrome* (ed. R. B. Denman), pp. 119-156. Berlin: Springer.
Tian, L., Stefanidakis, M., Ning, L., Van Lint, P., Nyman-Huttunen, H., Libert, C., Itohara, S., Mishina, M., Rauvala, H. and Gahmberg, C. G. (2007). Activation of NMDA receptors promotes dendritic spine development through MMP-mediated ICAM-5 cleavage. *J. Cell Biol.* **178**, 687-700.
Tocchi, A. and Parks, W. C. (2013). Functional interactions between matrix metalloproteinases and glycosaminoglycans. *FEBS J.* **280**, 2332-2341.
Uhlirova, M. and Bohmann, D. (2006). JNK- and Fos-regulated Mmp1 expression cooperates with Ras to induce invasive tumors in Drosophila. *EMBO J.* **25**, 5294-5304.
van Amerongen, R. (2012). Alternative Wnt pathways and receptors. *Cold Spring Harb. Perspect. Biol.* **4**, a007914.
Vautrin, J. (2010). The synaptomatrix: a solid though dynamic contact disconnecting transmissions from exocytotic events. *Neurochem. Int.* **57**, 85-96.
Wagh, D. A., Rasse, T. M., Asan, E., Hofbauer, A., Schwenkert, I., Dürrbeck, H., Buchner, S., Dabauvalle, M.-C., Schmidt, M., Qin, G. et al. (2006). Bruchpilot, a protein with homology to ELKS/CAST, is required for structural integrity and function of synaptic active zones in Drosophila. *Neuron* **49**, 833-844.
Wang, X. and Page-McCaw, A. (2014). A matrix metalloproteinase mediates long-distance attenuation of stem cell proliferation. *J. Cell Biol.* **206**, 923-936.
Wang, Q., Uhlirova, M. and Bohmann, D. (2010). Spatial restriction of FGF signaling by a matrix metalloprotease controls branching morphogenesis. *Dev. Cell* **18**, 157-164.
Wei, S., Xie, Z., Filenova, E. and Brew, K. (2003). Drosophila TIMP is a potent inhibitor of MMPs and TACE: similarities in structure and function to TIMP-3. *Biochemistry* **42**, 12200-12207.
Wilczynski, G. M., Konopacki, F. A., Wilczek, E., Lasiecka, Z., Gorlewicz, A., Michaluk, P., Wawrzyniak, M., Malinowska, M., Okulski, P., Kolodziej, L. R.

Development (2016) 143, 75-87 doi:10.1242/dev.124461

et al. (2008). Important role of matrix metalloproteinase 9 in epileptogenesis. *J. Cell Biol.* **180**, 1021-1035.

Wójtowicz, T., Brzda, P. and Mozrzymas, J. W. (2015). Diverse impact of acute and long-term extracellular proteolytic activity on plasticity of neuronal excitability. *Front. Cell. Neurosci.* **9**, 313.

Wu, Y., Belenkaya, T. Y. and Lin, X. (2010). Dual roles of Drosophila glypican Dally-like in Wingless/Wnt signaling and distribution. *Methods Enzymol.* **480**, 33-50.

Yan, D., Wu, Y., Feng, Y., Lin, S.-C. and Lin, X. (2009). The core protein of glypican Dally-like determines its biphasic activity in wingless morphogen signaling. *Dev. Cell* **17**, 470-481.

Yasunaga, K.-I., Kanamori, T., Morikawa, R., Suzuki, E. and Emoto, K. (2010). Dendrite reshaping of adult Drosophila sensory neurons requires matrix metalloproteinase-mediated modification of the basement membranes. *Dev. Cell* **18**, 621-632.

Zcharia, E., Jia, J., Zhang, X., Baraz, L., Lindahl, U., Peretz, T., Vlodavsky, I. and Li, J.-P. (2009). Newly generated heparanase knock-out mice unravel co-regulation of heparanase and matrix metalloproteinases. *PLoS ONE* **4**, e5181.

Zhang, L., Syed, Z. A., van Dijk Härd, I., Lim, J.-M., Wells, L. and Ten Hagen, K. G. (2014). O-glycosylation regulates polarized secretion by modulating Tango1 stability. *Proc. Natl. Acad. Sci. USA* **111**, 7296-7301.